Journal of ELECTRONIC MATERIALS, Vol. 46, No. 11, 2017
DOI: 10.1007/s11664-017-5701-8

Characterization and Electrochemical Performance at High Discharge Rates of Tin Dioxide Thin Films Synthesized by Atomic Layer Deposition

M.YU. MAXIMOV,[1] P.A. NOVIKOV,[1,4] D.V. NAZAROV,[1] A.M. RYMYANTSEV,[2] A.O. SILIN,[1] Y. ZHANG,[3] and A.A. POPOVICH[1]

1.—Peter the Great Saint-Petersburg Polytechnic University, Saint Petersburg, Russia 195221. 2.—Ioffe Institute, Saint Petersburg, Russia 195221. 3.—Hebei University of Technology, Tianjin Key Laboratory of Laminating Fabrication and Interface Control Technology for Advanced Materials, Tianjin 300401, China. 4.—e-mail: novikov.p.a@gmail.com

In this study, thin films of tin dioxide have been synthesized on substrates of silicon and stainless steel by atomic layer deposition (ALD) with tetraethyl tin and by inductively coupled remote oxygen plasma as precursors. Studies of the surface morphology by scanning electron microscopy show a strong dependence on synthesis temperature. According to the x-ray photoelectron spectroscopy measurements, the samples contain tin in the oxidation state +4. The thickness of the thin films for electrochemical performance was approximately 80 nm. Electrochemical cycling in the voltage range of 0.01–0.8 V have shown that tin oxide has a stable discharge capacity of approximately 650 mAh/g during 400 charge/discharge cycles with an efficiency of approximately 99.5%. The decrease in capacity after 400 charge/discharge cycles was around 5–7%. Synthesized SnO_2 thin films have fast kinetics of lithium ions intercalation and excellent discharge efficiency at high C-rates, up to 40C, with a small decrease in capacity of less than 20%. Specific capacity and cyclic stability of thin films of SnO_2 synthesized by ALD exceed the values mentioned in the literature for pure tin dioxide thin films.

Key words: Atomic layer deposition, Li-ion, tin dioxide, anode materials

INTRODUCTION

Lithium-ion batteries (LIBs) have for decades attracted enormous interest from industry and from the scientific community because of their high energy density and longer shelf life relative to other secondary battery technologies. Today, LIBs are the dominant power source for a myriad of types of portable electronic devices, which means that the development of next-generation electrode materials for LIBs is currently attracting intense attention from material scientists.[1] Tin dioxide is considered to be a promising anode material for LIBs because of its high theoretical specific capacity of 1491 mAh/g.[2,3] According to a few studies,[1,4] the following reversible redox reaction occurs in the Li/SnO_2 system:

$$SnO_2 + xLi^+ + xe^- \leftrightarrow Li_xSn + Li_2O$$
$$(0 \le x \le 4.4) \quad 0.05\text{–}2.5\,V.$$

It has been shown[5–7] that in a voltage range of 2.5–0.05 V, phase transitions take place that result in tin reduction with the further production of Li_xSn intermetallics. The theoretical capacity of SnO_2 ($\sim$790 mAh/g) corresponds to a $Li_{22}Sn_5$ intermetallic compound. However, in some cases,[5,6] the obtained specific capacity can exceed the theoretical value. It was shown,[1] that additional capacity was related to Li_2O production. It should be noted that the processes occurring during tin oxide-based

(Received March 30, 2017; accepted July 13, 2017; published online July 26, 2017)

anode cycling in a voltage range of 0.05–2.5 V are accompanied by a volume gain of the material that exceeds 200%. This volume gain may cause considerable damage to the internal structure, resulting in an obvious decrease in reversible capacity.[8,9] Therefore, it is essential to determine the voltage range where the stable reversible intercalation/deintercalation of lithium ions occurs. Also, various strategies have been proposed to resolve the abovementioned problems associated with SnO_2-based anodes, including, synthesis of low-dimensional materials (nanomaterials) such as hollow nanoparticles, nanorods, nanowires, nanosheets, and nanofilms. Such nanomaterials have better stability throughout multiple lithium insertion/removal processes, faster insertion/removal as a result of the shorter distance required for transporting lithium ions inside the material, and greater specific surface area.[10]

In recent years, researchers have given increasing attention to solid-state batteries, which are used for smart cards, chips with integrated power-supply units in portable devices, medical implants, etc.[11] At the moment, most such batteries use lithium as an anode. Use of tin oxide thin films as an anode is more promising[12] because of the absence of potential problems related to the safety and cycling of metal lithium.

One of the most advanced methods for obtaining thin films is the technology known as atomic layer deposition (ALD). ALD is based on consequent self-controlling heterogeneous chemical reactions that occur on the surface of a solid support[13,14] and allow applying coatings of various thickness with high precision. ALD is actively used for obtaining thin films of oxides,[13–15] including those of tin dioxide.[16] ALD provides a very low defect density in the material and gives a conformal deposition over highly corrugated and 3-dimensionally structured surfaces with nanometric precision in thickness. In the past, ALD in LIBs applications has been used to enable protective coatings (ex. Al_2O_3 layer) over electrode and electrolytes (separators) to improve the cycleability and suppress unwanted side reactions with an electrolyte counterpart.[17]

In this respect, we consider that ALD as a tool for synthesis of tin oxide thin films, which will be used as an anode for solid-state lithium-ion batteries, is especially relevant. For this reason, we have synthesized thin films of tin oxide using tetraethyl tin (TET). The resulting films were tested at extreme discharge speeds up to 40C.

MATERIALS AND METHODS

Samples of tin oxide thin film electrodes were obtained using a Picosun R-150 ALD system with the use of TET—$Sn(C_2H_5)_4$, CAS # 597-64-8 purity 99.999% and inductively coupled remote oxygen plasma as sources of tin and oxygen, respectively. The power of the plasma was 2500 W, and the frequency was 2.2 MHz. The application of the deposition technique was based on previous research.[18–20]

Optimization of the conditions for synthesis was performed using single-crystal silicon as a support. For further electrochemical study, tin dioxide thin films were deposited on the surface of 316SS stainless steel plates with diameters of 15 mm. The surface of the substrates was degreased and cleaned in acetone, ethyl alcohol, and deionized water at a temperature of 45–50°C in an ultrasonic bath. The cleaned plates were placed in a reactor; vacuum was created by pumping out up to 8 hPa. Synthesis was carried out at temperatures of 250°C and 300°C at least three times for each parameter to determine the reproducibility of film fabrication by ALD. To achieve the required pressure for the reagent vapor (around 10 hPa), the vessel with TET was heated up to 65°C. $Sn(C_2H_5)_4$ pulse time was 0.1 s, the purging time of high-purity nitrogen was 6 s, and the plasma processing time was 14 s. The number of ALD cycles for deposition on silicon and testing the technique was 450. For reliable measurement of the electrochemical properties of the films, the thickness cannot be less than 75–80 nm, so 1000 ALD cycles were run to coat the steel electrodes. The thickness of films was measured with the use of an “Ellipse 1891 SAG” spectral ellipsometer. The phase, element composition, and morphology of the films were studied by x-ray diffraction analysis (XRD) using Bruker D8 Discover, x-ray photoelectron spectroscopy (XPS) using Thermo Fisher Scientific Escalab 250Xi, and scanning electron microscopy (SEM) using Zeiss SUPRA 40VP.

The morphology and thickness of the films obtained on the steel surface were studied on the Cross-beam SEM workstation Zeiss AURIGA Laser. A protective carbon film was deposited with the use of a local gas injection system and with phenanthrene as a precursor. Cross-sections were made by a focused gallium ion beam. The parameters of the beam were as follows: accelerating voltage 30 kV; for the beam current: initial stage 4 A, intermediate stage 600 A, and final stage 50 A. The secondary electron signal was used to build images. The angle between the electron gun and the ion gun was 45°. Electrochemical studies were carried out in coin cell batteries (CR2032) relative to lithium metal with a TC-E918 Tinci electrolyte (1 M LiPF6 in EC:DMC = 1:1 vol.%) and a 2325 separator (Celgard). Assembly was made in a dry argon atmosphere in an Omni-Lab glove box (Vacuum Atmospheres). The current–voltage curves were measured using an Autolab PGSTAT302 N potentiostat (Metrohm) with a scanning rate of 0.1 mV/s in a voltage range from 0.05 V up to 3.0 V. To ensure reproducibility, at least five samples were used for each test. Electrochemical tests were conducted using a CT3008W-5V10 mA charge/discharge stand (Neware) in a voltage range from 0.8 V

to 0.05 V and discharge current densities from 25 μA/cm^2 to 2000 μA/cm^2 (C-rate scale: from 0.5C to 40C, respectively).

RESULTS AND DISCUSSION

The experimental results acquired by the spectroscopic ellipsometry method show that reliable processing of the experimental data for the sample obtained at 250°C is impossible in the case of a simple multilayer "Si/SiO_2/SnO_2" optical model, which includes a silicon substrate, a natural silicon oxide sub-layer, and a tin dioxide continuous layer. Satisfactory consistency of the calculated and experimental data were achieved when a more complex "Si/SiO_2/SnO_2/rough SnO_2" model was used, where rough SnO_2 was added. This layer is not continuous and reflects the roughness of the surface. It should be noted that the latter model was also successfully used for the sample obtained at 300°C. Inapplicability of the simple multilayer model for ALD tin oxide thin films obtained at temperatures below 200°C has been demonstrated previously.[20] The results of the processing of experimental data are presented in Table I. The total average thickness of the film obtained at 250°C is almost twice that of the sample obtained at 300°C. Therewith, the difference is caused primarily by the thickness of the rough layer. According to the ellipsometry data, an assumption can be made that the 300°C sample contains a continuous and relatively smooth film, whereas the 250°C sample is marked by considerable roughness.

The assumption concerning the difference in morphology of the films was confirmed after the samples were examined by scanning electron microscopy. The SEM images (Fig. 1) show that the sample obtained at 250°C has a complex structure and a well-developed relief. According to both in-plane and cross-section images, the films consist of separate structures. Based on the cross-section view, the film obtained at 300°C is denser and more continuous and homogenous than that formed at 250°C. However, the in-plane view clearly shows granular structures with diameters of 10–20 nm, which fully cover the surface of the sample. The estimated thicknesses of the films according to the cross-section SEM images are 70–80 nm and 30–35 nm, respectively; meanwhile, the growth rates of the films obtained at 250°C and 300°C per one ALD cycle are ~0.17 nm and ~0.07 nm, respectively.

In-plane and cross-section images were also obtained for the films deposited on steel substrates (Fig. 2). The cross-section images were taken after cross-section cuts were made with a focused beam of gallium ions. The in-plane view shows that the difference in morphology of the samples is not as dramatic as that in the films obtained on the surface of silicon, but it should be noted that the sample obtained at 250°C has a more distinctive relief. Difference in temperature dependent morphology changes of the films deposited on different supports can be explained by the roughness factor. Silicon has a minimal roughness (about 1 nm) and this factor is negligible. In the case of stainless steel support, the roughness is the more important factor, which influences morphology. Unfortunately, the cross-section images do not allow judging of the morphology of the films, as it is disturbed by the beam of gallium ions. However, the cross-section view makes it possible to estimate the thickness and growth rate (GPC). For the sample obtained at 250°C, the thickness was approximately 83 nm (GPC = 0.083 nm), while for the 300°C sample, it was 78 nm (GPC = 0.078 nm). It should be noted that particles of the films on steel substrates had a larger size than those of the films on silicon. Thus, the type of substrate has a strong impact on both the morphology and growth rate of tin dioxide films.

According to the XRD data shown in Fig. 3, the tin oxide thin films synthesized at temperatures of 250°C and 300°C have an amorphous structure. However, it should be noted that in the XRD data for the sample obtained at 300°C, there are greatly broadened peaks, which may confirm that a new phase is beginning to crystallize. The diffraction peaks of the two samples correspond to reflection planes of (110), (101), (211), and (220), which are associated with cassiterite (JCPDS file no. 41-1445).

Figure 4 displays the high-resolution XPS spectra of Sn3d and O1 s levels and the simulated data obtained by decomposition of the observed peaks. The figures demonstrate that the Sn3d level contains only one component, with the peak value maxima equal to 486.6 eV and 495 eV, common for Sn^{4+},[15] while the O1s peak can be decomposed into two components with maxima at approximately 530.4 eV and 531.8 eV, which correspond to O^{2-}-Sn bonds and surface hydroxyls, respectively.[15]

The electrochemical characteristics of the tin oxide thin films were studied for samples with thicknesses of approximately 80 nm obtained on the

Table I. Ellipsometry results

Temperature	Optical model	SnO_2 thickness, nm	Rough SnO_2 thickness, nm	SnO_2 content in rough SnO_2, %	Total average thickness, nm
250	Si/SiO_2/SnO_2/rough SnO_2	15.0	55.0	33	70
300	Si/SiO_2/SnO_2/rough SnO_2	27.2	8.7	70	35.9
300	Si/SiO_2/SnO_2	33.3	–	–	33.3

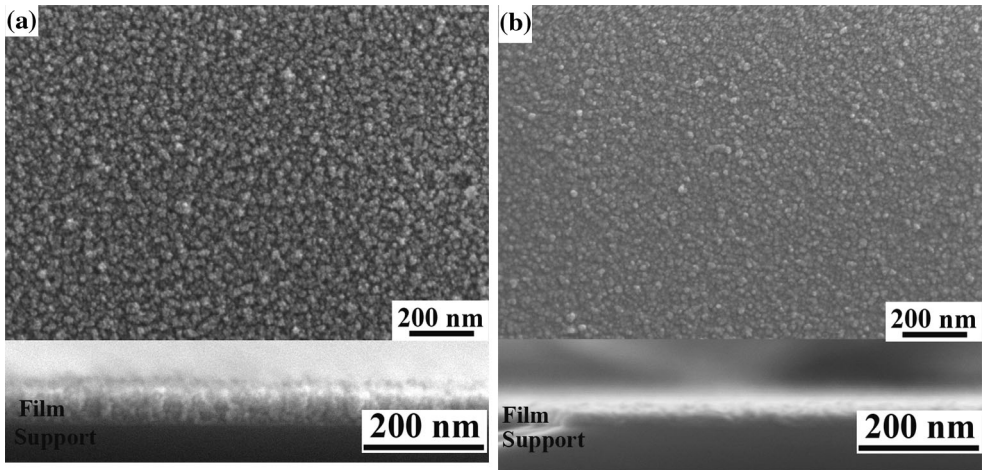

Fig. 1. SEM images (in plane and cross-section) of samples of tin dioxide thin films on silicon obtained at (a) 250°C and (b) 300°C.

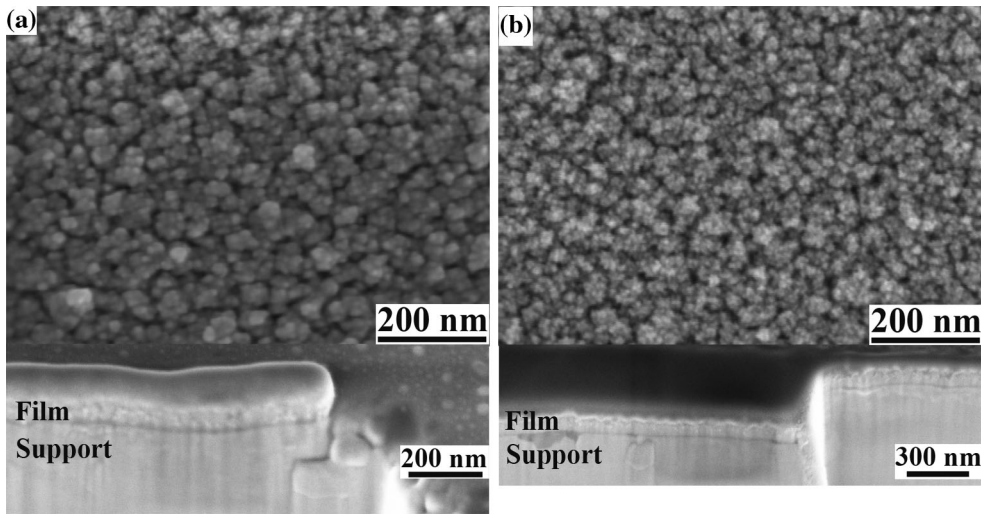

Fig. 2. SEM images of tin dioxide thin films on steel obtained at (a) 250°C and (b) 300°C. Cross-section images were acquired at a 45° inclination of the sample with respect to the normal.

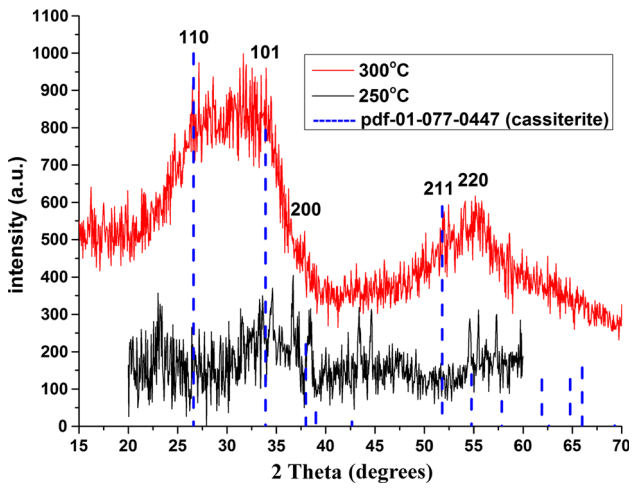

Fig. 3. XRD data for tin oxide thin films obtained at 250°C and 300°C.

surface of 316SS stainless steel plates. Cyclic voltammetry (CV) was used to reveal phase transformations in the obtained samples, define the optimal voltage range to study the cyclic stability of the material and determine the influence of the substrate on obtained capacity. The results of the studies are given in Fig. 5.

According to CV curves for stainless steel wafers with electrolyte, influence of this substrate and electrolyte can be neglected.

Three peaks are clearly seen in tin dioxide cycling, which correspond to the following transformations[3]:

$$SnO_2 + 2Li^+ + 2e^- \leftrightarrow SnO + Li_2O\ 1.7{-}2\,V, \quad (1)$$

$$SnO + 2Li^+ + 2e^- \leftrightarrow Sn + 2Li_2O\ 0.9{-}1.3\,V, \quad (2)$$

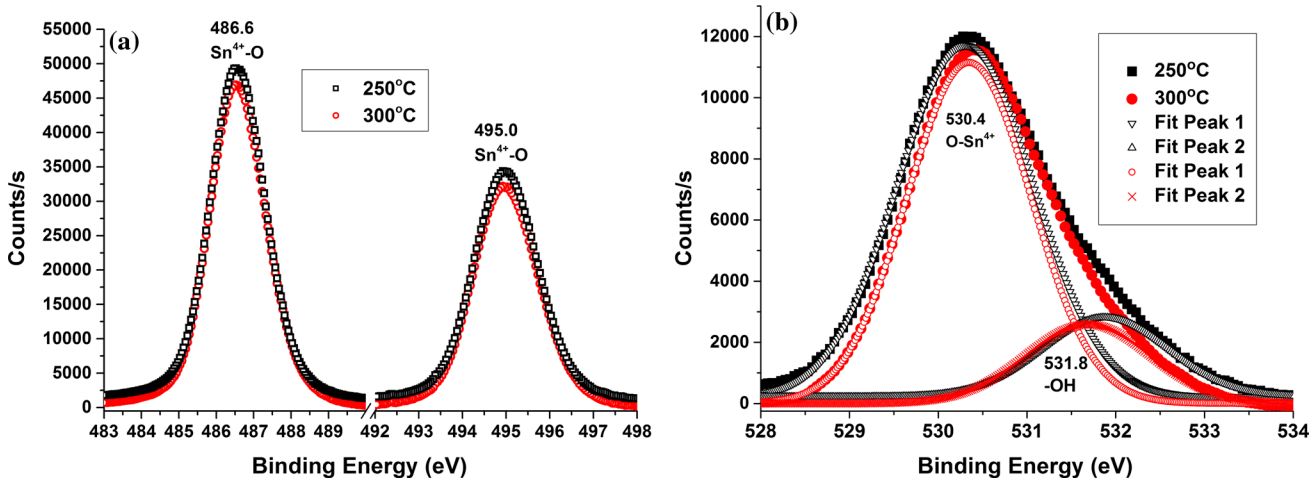

Fig. 4. XPS spectra of tin oxide films synthesized at 250°C and 300°C (a) XPS spectra of Sn3d level and (b) XPS spectra of O1s level.

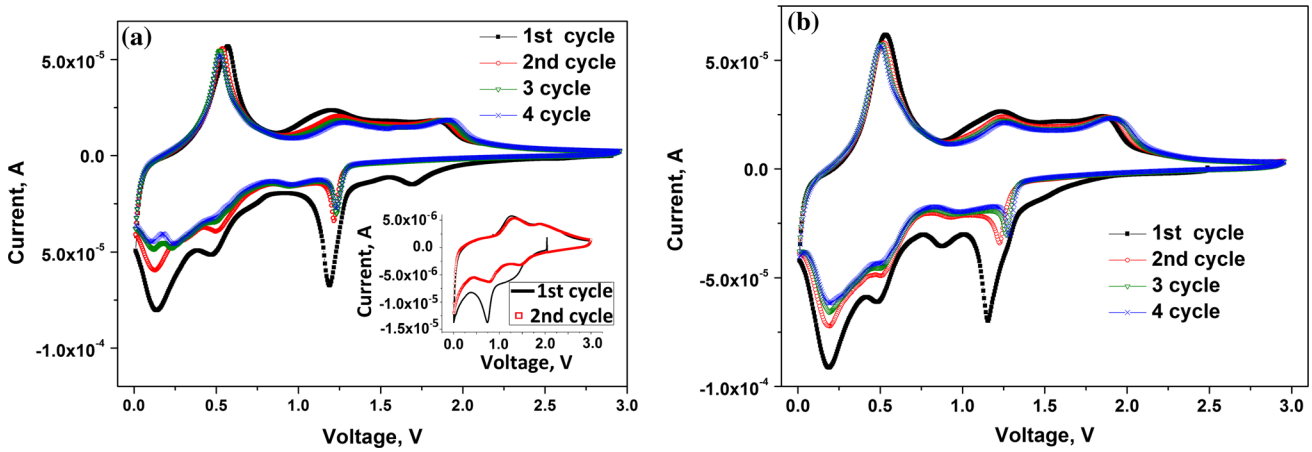

Fig. 5. Cyclic voltammogram curves for tin oxide thin films obtained at (a) 250°C and (b) 300°C. Inset presents CV for 316SS stainless steel wafers with electrolyte.

$$\mathrm{Sn} + \mathrm{xLi}^{+} + \mathrm{xe}^{-} \leftrightarrow \mathrm{Li_xSn}\ (0 \le \mathrm{x} \le 4.4)\ 0.05\text{–}0.8\ \mathrm{V}. \quad (3)$$

The results for samples obtained at 250°C and 300°C do not show a noticeable difference. According to the observed results and the research reported in paper,[3] it can be concluded that the most stable potential window for researching the cyclic stability of SnO_2-based materials and for obtaining maximum efficiency is 0.05–0.8 V. Earlier we also[18] studied the cyclic stability of tin oxide thin films at various voltage ranges. It has been shown that the most optimal regime for cycling is a voltage range of 0.05–0.8 V.

Because of their small thickness and good conformability, thin films have drawn interest in the field of fast discharge. Tin dioxide thin films should have sufficiently fast kinetics and should be able to work at high C-rates. According to this idea, tests with C-rates up to 40C were performed. The electrochemical experiments were conducted using the following scheme: 1C—10 cycles; 0.5C—5 cycles; 1C—5 cycles; 2C—5 cycles; 3C—5 cycles; 4C—5 cycles; 5C—5 cycles; 6C—5 cycles; 8C—5 cycles; 10C—5 cycles; 12C—5 cycles; 1C—5 cycles; 0.5C—5 cycles; 1C—5 cycles; 14C—5 cycles; 16C—5 cycles; 18C—5 cycles; 20C—5 cycles; 24C—5 cycles; 28C—5 cycles; 30C—5 cycles; 40C—5 cycles; and 1C—5 cycles.

The effect of current density on the specific capacity of tin dioxide thin films obtained at 250°C and 300°C is presented in Fig. 6.

Figure 6a shows that the difference in the reversible capacity for the samples synthesized at 250°C and 300°C is approximately 20%. Figure 6b shows a decrease in capacity with increasing current density. The maximal specific capacity was fixed at 0.5C and set as 100%. The following percentages were calculated from the specific capacity at the set C-rate.

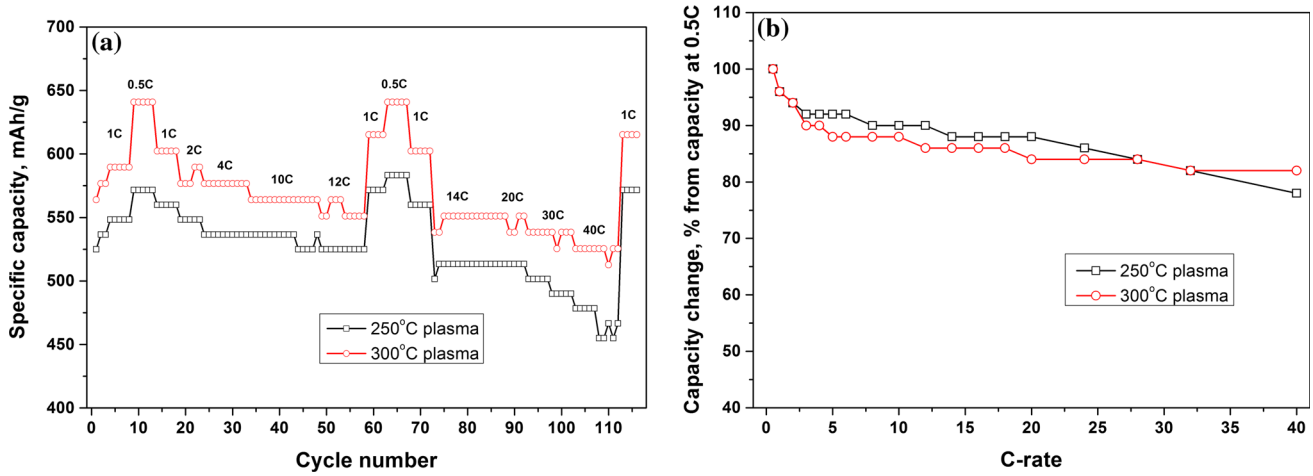

Fig. 6. Effect of current density on specific capacity of tin oxide films (IV) obtained at 250°C and 300°C. Specific capacity versus cycle number (a), capacity change versus current density (b).

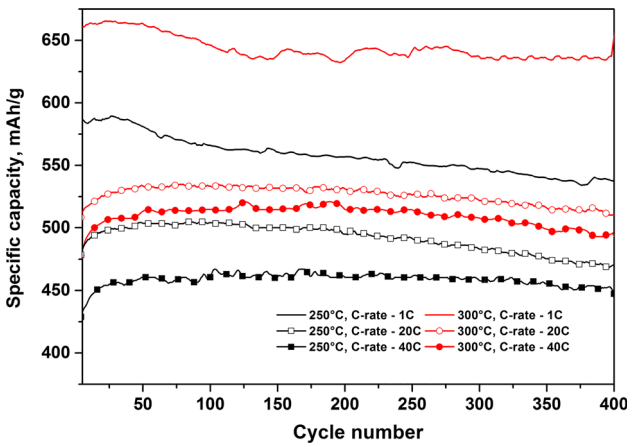

Fig. 7. Cyclic stability of tin oxide thin films (IV) obtained at 250°C and 300°C depending on current density.

Figure 6b shows that there is a rapid drop in capacity from 100% to 90% as the current density increases from 0.5C to 3–5C for both samples. Further changes occur gradually, from 90% to 80%, with a C-rate increase. Difference between samples is observed at high C-rate (20–40). The specific capacity of the samples synthesized at 300°C decreased slowly at this range. For samples synthesized at 250°C, with every increase of the current density over 20C, the capacity was reduced proportionally to the current density and significantly faster than for the sample 300°C. This may be due to the higher density of tin oxide films obtained at higher temperature (Figs. 1 and 2).

It can be concluded that the prepared SnO_2 thin films have fast kinetics of lithium ions intercalation and excellent discharge efficiency at high C-rates, up to 40C, with a small decrease in capacity of less than 20%.

The cyclic stability of the obtained samples of tin dioxide thin films has been tested for more than 400 charge/discharge cycles (Fig. 7).

According to the obtained results, the Coulomb efficiency throughout of all the tests is 99.0–99.7%, apart from the first cycle, where the efficiency is 30–35%. The cause of the low efficiency during the first cycle is the potential range selected at cycling. On top, it is limited by 0.8 V, i.e., at the first charge, reactions Eqs. 1–3 occur, and at the first discharge, the same as at all further charges and discharges, only reaction Eq. 3 takes place. The decrease in capacity after 400 charge/discharge cycles is approximately 5–7% for 300°C samples. For 250°C samples, degradation is approximately 10–15%.

The capacity of tin dioxide samples synthesized at 300°C is therefore higher. This may be due to the fact that the films obtained at 300°C are denser, more homogeneous, and have “crystal nuclei”. Because the specific capacities of the thin films were estimated on the basis of cassiterite density, higher density corresponds to lower specific capacity.

The samples are stable with increasing C-rate, but the decrease in specific capacity for 300°C samples with increasing C-rate from 20C to 40C is lower than that for 250°C samples, at 5–7% and 12–16%, respectively. Thin films synthesized at lower temperature are more sensitive to an increase in the discharge current density. This may be due to the fact that 250°C samples are porous and less dense.

The results obtained in this work with respect to specific capacity and cyclic stability at current densities up to 40C for thin films of SnO_2 synthesized by ALD have not been previously discussed in the literature. Most promising electrochemical performancesof tin dioxide has been obtained from studies of composite materials: SnO_2-graphene or SnO_2-carbon nanotubes. It should be taken into account that the increase in specific capacity may be

caused by the formation of lithium compounds with carbon (LiC_6). The electrochemical characteristics of tin oxide deposited on graphene layers by ALD presented in[21] are approximately 700 mAh/g during 160 cycles at 1C. In,[22] the authors demonstrated properties of tin oxide doped by other electrochemically active elements (Co, Fe) and mixed with graphene.

CONCLUSIONS

ALD was used to deposit tin dioxide using TET and oxygen plasma for a high-performance anode material. Using oxygen plasma as the oxidizer allowed us to deposit coatings over a wide range of temperatures, but the temperature greatly affected the film's morphology structure. The films deposited below 300°C were amorphous. XPS measurements showed that the prepared samples contained tin in the +4 oxidation state. Under the optimal deposition conditions, tin oxide films were deposited on steel supports at 250°C and 300°C.

The obtained SnO_2 films exhibited very stable cycling electrochemical performance during more than 400 charge/discharge cycles, with a Coulombic efficiency of over 99% in a voltage range of 0.05–0.8 V at current densities up to 40C. The capacity decrease was approximately 5–7%. The thin films with "crystal nuclei" showed a specific capacity above 650 mAh/g without being doped by other electrochemically active elements (Co, Fe) or mixed with graphene. Densification of the films had a positive influence on the specific capacity at high C-rates. According to the experimental data, tin dioxide thin films have sufficiently fast kinetics and are able to hold fast C-rates without any great loss of specific capacity.

The samples are stable with increasing C-rate, but a decrease in specific capacity for 300°C samples with an increase in the C-rate from 20C to 40C is lower than that for 250°C samples, at 5–7% and 12–16%, respectively. Synthesized SnO_2 thin films have fast kinetics of lithium ions intercalation and excellent discharge efficiency at high C-rates, up to 40C, with a small decrease in capacity of less than 20%.

ACKNOWLEDGEMENT

This research was conducted using the equipment of the resource centers of the Research Park of the St. Petersburg State University "Innovative Technologies of Composite Nanomaterials", "Centre for Physical Methods of Surface Investigation", "Centre for x-ray Diffraction Studies", and "Nanotechnology Interdisciplinary Centre".

REFERENCES

1. J.S. Chen, L.A. Archer, and X.W. Lou, *J. Mater. Chem.* (2011). doi:10.1039/c0jm04163g.
2. C. Jiajun, *Materials* (2013). doi:10.3390/ma6010156.
3. S.Y. Lee, K.Y. Park, W.S. Kim, S. Yoon, S.H. Hong, K. Kang, and M. Kim, *Nano Energy* (2016). doi:10.1016/j.nanoen.2015.10.026.
4. H.B. Wu, J.S. Chen, H.H. Huey, and X.W. Lou, *Nanoscale* (2012). doi:10.1039/c2nr11966h.
5. V. Aravindana, K.B. Jinesha, R.R. Prabhakara, V.S. Kalea, and S. Madhavi, *Nano Energy* (2013). doi:10.1016/j.nanoen.2012.12.007.
6. K. Kravchyk, L. Protesescu, M.I. Bodnarchuk, F. Krumeich, M. Yarema, M. Walter, C. Guntlin, and V.K. Maksym, *J. Am. Chem. Soc.* (2013). doi:10.1021/ja312604r.
7. A.G. Morachevskii, *Russ. J. Appl. Chem.* (2015). doi:10.1134/S1070427215070010.
8. D. Larcher, S. Beattie, M. Morcrette, K. Edström, J.C. Jumas, and J.M. Tarascon, *J. Mater. Chem.* (2007). doi:10.1039/B705421C.
9. J.Y. Huang, L. Zhong, C.M. Wang, J.P. Sullivan, W. Xu, L.Q. Zhang, S.X. Mao, N.S. Hudak, X.H. Liu, A. Subramanian, H. Fan, L. Qi, A. Kushima, and J. Li, *Science* (2010). doi:10.1126/science.1195628.
10. P.G. Bruce, B. Scrosati, and J.M. Tarascon, *Angew. Chem. Int. Ed.* (2008). doi:10.1002/anie.200702505.
11. S.H. Jee, S.H. Lee, D.-J. Kim, J.-Y. Kwak, S.-C. Nam, and Y.S. Yoon, *Jpn. J. Appl. Phys.* (2012). doi:10.1143/JJAP.51.085803.
12. S.C. Jun, W. Xiong, and D. Lou, *Small* (2013). doi:10.1002/smll.201202601.
13. S.M. George, *Chem. Rev.* (2010). doi:10.1021/cr900056b.
14. M. Leskela and M. Ritala, *Angew. Chem. Int. Ed.* (2003). doi:10.1002/anie.200301652.
15. J. Szuber, G. Czempik, R. Larciprete, D. Koziej, and B. Adamowicz, *Thin Solid Films* (2001). doi:10.1016/S0040-6090(01)00982-8.
16. D.V. Nazarov, N.P. Bobrysheva, O.M. Osmolovskaya, M.G. Osmolovsky, and V.M. Smirnov, *Rev. Adv. Mater. Sci.* 40, 262 (2015).
17. A.A. Popovich, M.Yu. Maximov, A.M. Rumyantsev, and P.A. Novikov, *Russ. J. Appl. Chem.* (2015). doi:10.1134/S1070427215050274.
18. A.A. Popovich, M.Yu. Maximov, P.A. Novikov, A.O. Silin, D.V. Nazarov, and A.M. Rumyantsev, *Russ. J. Appl. Chem.* (2016). doi:10.1134/S1070427216040236.
19. D.V. Nazarov, M.Yu. Maximov, P.A. Novikov, and A.A. Popovich, *J. Vac. Sci. Technol., A* (2017). doi:10.1116/1.4972554.
20. A.A. Popovich, M.Yu. Maximov, D.V. Nazarov, and P.A. Novikov, *Russ. J. Appl. Chem.* (2016). doi:10.1134/S1070427216050190.
21. X. Li, X. Meng, J. Liu, D. Geng, Y. Zhang, M.N. Banis, Y. Li, J. Yang, R. Li, X. Sun, M. Cai, and M.W. Verbrugge, *Adv. Funct. Mater.* (2012). doi:10.1002/adfm.201101068.
22. Z. Yang, L. Xifei, Y. Bo, X. Dongbin, L. Dejun, S. Lawes, and X. Sun, *Adv. Energy Mater.* (2016). doi:10.1002/aenm.201502175.